Article

Light-Controlled Supramolecular Helicity of a Liquid Crystalline Phase Using a Helical Polymer Functionalized with a Single Chiroptical Molecular Switch

Dirk Pijper, Mahthild G. M. Jongejan, Auke Meetsma, and Ben L. Feringa

J. Am. Chem. Soc., **2008**, 130 (13), 4541-4552 • DOI: 10.1021/ja711283c

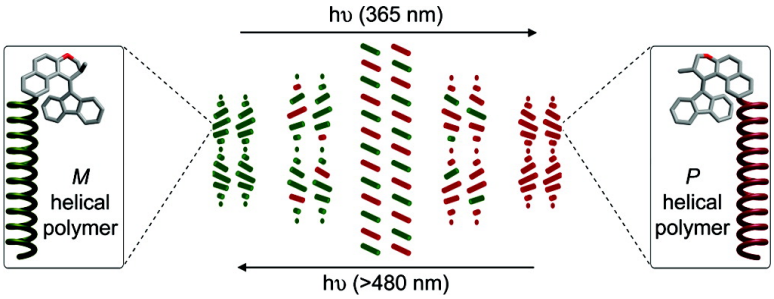

More About This Article

Additional resources and features associated with this article are available within the HTML version:

- Supporting Information
- Links to the 11 articles that cite this article, as of the time of this article download
- Access to high resolution figures
- Links to articles and content related to this article
- Copyright permission to reproduce figures and/or text from this article

View the Full Text HTML

J|A|C|S
ARTICLES
Published on Web 03/12/2008

Light-Controlled Supramolecular Helicity of a Liquid Crystalline Phase Using a Helical Polymer Functionalized with a Single Chiroptical Molecular Switch

Dirk Pijper, Mahthild G. M. Jongejan, Auke Meetsma, and Ben L. Feringa*

Department of Organic and Molecular Inorganic Chemistry, Stratingh Institute, University of Groningen, Nijenborgh 4, 9747 AG, Groningen, The Netherlands

Received December 20, 2007; Revised Manuscript Received January 30, 2008 ; E-mail: b.l.feringa@rug.nl

Abstract: Control over the preferred helical sense of a poly(*n*-hexyl isocyanate) (PHIC) by using a single light-driven molecular motor, covalently attached at the polymer's terminus, has been accomplished in solution via a combination of photochemical and thermal isomerizations. Here, we report that after redesigning the photochromic unit to a chiroptical molecular switch, of which the two states are thermally stable but photochemically bistable, the chiral induction to the polymer's backbone is significantly improved and the handedness of the helical polymer is addressable by irradiation with two different wavelengths of light. Moreover, we show that the chiral information is transmitted, via the macromolecular level of the polyisocyanate, to the supramolecular level of a lyotropic cholesteric liquid crystalline phase consisting of these stiff, rodlike polymers. This allows the magnitude and sign of the supramolecular helical pitch of the liquid crystal film to be fully controlled by light.

Introduction

The transmission of chiral information from the molecular to the macro- and supramolecular level[1] is a powerful mechanism used by nature in the controlled self-assembly of complex macromolecular superstructures such as proteins and DNA.[2] In artificial systems, it offers the opportunity to control the properties of materials in a dynamic and reversible manner. In particular, it has been demonstrated that smart materials can be triggered to alter their properties upon switching of chiral structures at the molecular level.[3] The amplification of chirality has been realized with several dynamically helical systems, e.g., chiral aggregates and gels,[4] synthetic helical foldamers,[5] or polymers.[6] Liquid crystals (LCs) are especially suitable as a host material for this purpose, due to their sensitivity to small molecular chiral perturbations.[7]

Whereas only a slight orientational order is present in an ordinary nematic LC matrix, the cholesteric (or chiral nematic) LC phase is characterized by an additional change of the direction of the individual mesogens in a helical fashion perpendicular to the original director. The resulting large supramolecular chiral organization is indicated by the sign and magnitude of the cholesteric pitch (p), which is the distance along the helix axis across which the director rotates a full 360°. The nematic-to-cholesteric phase transition can be induced by the addition of certain chiral dopant molecules to an LC formed by achiral mesogens.[8] The development of switchable dopants, which can change shape under the influence of an external stimulus (for instance light or heat) and consequently alter their chiral induction toward the LC medium, holds great promise toward future application.[9] A series of chiroptical molecular switches[10] and light-driven molecular motors based on sterically overcrowded alkenes[11] developed in our laboratories proved to be excellent photoswitchable dopants, due to the inversion of the intrinsic helicity of the molecules involved with the

(1) (a) Feringa, B. L.; Van Delden, R. A. *Angew. Chem., Int. Ed.* **1999**, *38*, 3418−3438. (b) Crego-Calama, M., Reinhoudt, D. N., Eds. *Supramolecular Chirality*; *Top. Curr. Chem.* **2006**, *265*.

(2) (a) Schulz, G. E.; Schirmer, R. H. *Principles of Protein Structure*; Springer-Verlag: New York, 1979. (b) Saenger, W. *Principles of Nucleic Acid Structure*; Springer-Verlag: New York, 1984.

(3) (a) De Jong, J. J. D.; Hania, P. R.; Pugžlys, A.; Lucas, L. N.; De Loos, M.; Kellogg, R. M.; Feringa, B. L.; Duppen, K.; Van Esch, J. H. *Angew. Chem., Int. Ed.* **2005**, *44*, 2373−2376. (b) Eelkema, R.; Pollard, M. M.; Vicario, J.; Katsonis, N.; Ramon, B. S.; Bastiaansen, C. W. M.; Broer, D. J.; Feringa, B. L. *Nature* **2006**, *440*, 163. (c) Eelkema, R.; Pollard, M. M.; Katsonis, N.; Vicario, J.; Broer, D. J.; Feringa, B. L. *J. Am. Chem. Soc.* **2006**, *128*, 14397−14407. (d) Uchida, K.; Sukata, S.; Matsuzawa Y.; De Jong, J. J. D.; Katsonis, N.; Kojima, Y.; Nakamura, S.; Areephong, J.; Meetsma, A.; Feringa, B. L. *Chem. Commun.* **2008**, 326−328.

(4) (a) Engelkamp, H.; Middelbeek, S.; Nolte, R. J. M. *Science* **1999**, *284*, 785−788. (b) Hirschberg, J. H. K. K.; Brunsveld, L.; Ramzi, A.; Vekemans, J. A. J. M.; Sijbesma, R. P.; Meijer, E. W. *Nature* **2000**, *407*, 167−170. (c) Fenniri, H.; Deng, B.-L.; Ribbe, A. E. *J. Am. Chem. Soc.* **2002**, *124*, 11064−11072. (d) De Jong, J. J. D.; Lucas, L. N.; Kellogg, R. M.; Van Esch, J. H.; Feringa, B. L. *Science* **2004**, *304*, 278−281. (e) Eelkema, R.; Feringa, B. L. *J. Am. Chem. Soc.* **2005**, *127*, 13480−13481.

(5) Hill, D. J.; Mio, M. J.; Prince, R. B.; Hughes, T. S.; Moore, J. S. *Chem. Rev.* **2001**, *101*, 3893−4011.

(6) (a) Green, M. M.; Peterson, N. C.; Sato, T.; Teramoto, A.; Cook, R.; Lifson, S. *Science* **1995**, *268*, 1860−1866. (b) Yashima, E.; Matsushima, T.; Okamoto, Y. *J. Am. Chem. Soc.* **1995**, *117*, 11596−11597. (c) Maeda, K.; Yashima, E. *Top. Curr. Chem.* **2006**, *265*, 47−88. (d) Pijper, D.; Feringa, B. L. *Angew. Chem., Int. Ed.* **2007**, *46*, 3693−3696.

(7) (a) Huck, N. P. M.; Jager, W. F.; De Lange, B.; Feringa, B. L. *Science* **1996**, *273*, 1686−1688. (b) Collings, P. J., Patel, J. S., Eds. *Handbook of Liquid Crystal Research*; Oxford University Press: New York, Oxford, 1997. (c) Kitzerow, H.-S., Bahr, C., Eds. *Chirality in Liquid Crystals*; Springer-Verlag: New York, 2001.

(8) (a) Solladié, G.; Zimmermann, R. G. *Angew. Chem., Int. Ed.* **1984**, *23*, 348−362. (b) For a comprehensive overview of recently developed chiral dopant systems, see: Eelkema, R.; Feringa, B. L. *Org. Biomol. Chem.* **2006**, *4*, 3729−3745.

(9) (a) Tamaoki, N. *Adv. Mater.* **2001**, *13*, 1135−1147. (b) Ichimura, K. *Chem. Rev.* **2000**, *100*, 1847−1873.

isomerization steps of these systems. This concept was extended to chiral amplification by irradiation with circularly polarized light (CPL) of a nematic LC host doped with a racemic mixture of a chiroptical switch, resulting in deracemization of the switch, consequently generating a cholesteric phase.[7a] The use of light-driven molecular motors as the chiral guests led to the development of light addressable dopant−LC mixtures with pitches short enough to reflect visible light. The thermal and photochemical isomerizations of these motors led to reversible color changes of the LC film, yielding a system which possesses the basic requirements to generate addressable color pixels covering the full visible spectrum, potentially useful in future generation LC displays.[12] Irradiation of a molecular motor doped cholesteric LC even led to a unidirectional rotational reorganization of the surface texture of an LC film.[3b,c]

Besides these solvent-free thermotropic LC systems, there are many solvent−solute systems, where aggregation of the solutes at sufficiently high concentration leads to liquid crystallinity. Rigid rodlike polymers are well-known to form such a lyotropic LC phase.[7b] The photoinduced trans-to-cis isomerization of photochromic azobenzene groups introduced in the side chains of, for instance, copolyacrylates generally causes a disruption of the nematic LC phase, leading to a large change in birefringence.[13] Furthermore, CPL irradiation has been shown to lead to a long-range helical arrangement of the azobenzenes,[14] an effect that could be further amplified by a supramolecular chiral organization in polymeric LCs.[15] A series of polymeric LCs with photochromic switch units bearing a chiral pendant group, either covalently attached to the polymer side chains or seeded as a dopant in the LC material, were used to achieve photochemically induced changes in the cholesteric pitch.[16]

An intriguing class of rigid, LC-forming polymers are the polyisocyanates.[6a,17] The backbone of these polymers adopts a helical conformation, of which the equal amounts of left- and right-handed helical conformations dynamically interconvert. A small chiral induction can lead to a strong preference for one helical twist sense, due to the strong cooperativity of the monomeric units in the helical conformation and the resulting infrequency of helix reversals along the polymer chain. Amplification of chirality has been demonstrated with these polymers taking advantage of the "sergeants-and-soldiers"[18] and "majority-rules"[19] effects, and even by the substitution in each side chain of one hydrogen atom by a deuterium atom.[20] The transformation of a nematic lyotropic LC formed by poly(*n*-hexyl isocyanate) to the cholesteric state was also demonstrated by the addition of both various chiral small molecules and optically active polyisocyanates as dopants.[21] In an elegant approach toward switching of the helicity, Green and co-workers employed a polyisocyanate bearing structurally different chiral side chains, which compete with each other favoring a left- and right-handed helical sense of the polymer backbone.[22] Since the chiral bias of the competing units depends on temperature in different ways, the polymer was shown to switch its helical conformation between left- and right-handed as a function of temperature.[23] With the use of these temperature-dependent helicity-switchable polyisocyanates, also the helical pitch and twist sense of a cholesteric lyotropic LC formed by these polymers could be controlled thermally.[22b] The introduction of azobenzene photochromic groups containing two stereogenic centers in the side chains of a copolyisocyanate allowed the photochemically induced transition of excess *M* to *P* helicity of the polymer backbone in dilute solution.[24] As the chiral induction of the switch units toward the polymer backbone depends on a subtle interplay between the different components (the stereogenic centers do not change upon photoisomerization), the ability of switching of macromolecular helicity with these systems has proven to be rather sensitive to various parameters.[25] Furthermore, switching of the helical pitch of a lyotropic cholesteric LC formed by these azobenzene-functionalized polyisocyanates has not been demonstrated, although one example has been published in which the helical pitch could only be slightly altered in a reversible way.[16d] Also by irradiating an axially chiral bicyclic ketone moiety with CPL, introduced in the side chains of a copolyisocyanate, the preferred handedness of the polymer's backbone was switched in dilute solution.[26]

In all these photoswitchable polymeric systems, the chiral information of multiple photochromic switches randomly dis-

(10) (a) Jager, W. F.; De Jong, J. C.; De Lange, B.; Huck, N. M. P.; Meetsma, A.; Feringa, B. L. *Angew. Chem., Int. Ed.* **1995**, *34*, 348−350. (b) Feringa, B. L.; Huck, N. M. P.; Schoevaars, A. M. *Adv. Mater.* **1996**, *8*, 681−683. (c) Feringa, B. L.; Van Delden, R. A.; Koumura, N.; Geertsema, E. M. *Chem. Rev.* **2000**, *100*, 1789−1816.

(11) (a) Koumura, N.; Zijlstra, R. W. J.; Van Delden, R. A.; Harada, N.; Feringa, B. L. *Nature* **1999**, *401*, 152−155. (b) Koumura, N.; Geertsema, E. M.; Meetsma, A.; Feringa, B. L. *J. Am. Chem. Soc.* **2000**, *122*, 12005−12006. (c) Koumura, N.; Geertsema, E. M.; Van Gelder, M. B.; Meetsma, A.; Feringa, B. L. *J. Am. Chem. Soc.* **2002**, *124*, 5037−5051.

(12) (a) Van Delden, R. A.; Koumura, N.; Harada, N.; Feringa, B. L. *Proc. Natl. Acad. Sci. U.S.A.* **2002**, *99*, 4945−4949. (b) Van Delden, R. A.; Van Gelder, M. B.; Huck, N. P. M.; Feringa, B. L. *Adv. Funct. Mater.* **2003**, *13*, 319−324. (c) Eelkema, R.; Feringa, B. L. *Chem. Asian J.* **2006**, *1*, 367−369.

(13) (a) Natansohn, A.; Rochon, P. *Chem. Rev.* **2002**, *102*, 4139−4175. (b) Ikeda, T. *J. Mater. Chem.* **2003**, *13*, 2037−2057.

(14) Some amount of linear polarization in the CPL, essentially leading to elliptically polarized light, appeared to be required, see: (a) Kim, M.-J.; Shin, B.-G.; Kim, J.-J.; Kim, D.-Y. *J. Am. Chem. Soc.* **2002**, *124*, 3504−3505. (b) Kim, M.-J.; Yoo, S.-J.; Kim, D.-Y. *Adv. Funct. Mater.* **2006**, *16*, 2089−2094.

(15) (a) Nikolova, L.; Nedelchev, L.; Todorov, T.; Petrova, T.; Tomova, N.; Dragostinova, V.; Ramanujam, P. S.; Hvilsted, S. *Appl. Phys. Lett.* **2000**, *77*, 657−659. (b) Iftime, G.; Labarthet, F. L.; Natansohn, A.; Rochon, P. *J. Am. Chem. Soc.* **2000**, *122*, 12646−12650. (c) Wu, Y.; Natansohn, A.; Rochon, P. *Macromolecules* **2004**, *37*, 6801−6805.

(16) (a) Brehmer, M.; Lub, J.; Van de Witte, P. *Adv. Mater.* **1998**, *10*, 1438−1441. (b) Campbell, S.; Lin, Y.; Muller, U.; Chien, L.-C. *Chem. Mater.* **1998**, *10*, 1652−1656. (c) Bobrovsky, A. Y.; Boiko, N. I.; Shibaev, V. P.; Springer, J. *Adv. Mater.* **2000**, *12*, 1180−1183. (d) Mruk, R.; Zentel, R. *Macromolecules* **2002**, *35*, 185−192. (e) Shibaev, V.; Bobrovsky, A.; Boiko, N. *Prog. Polym. Sci.* **2003**, *28*, 729−836.

(17) Green, M. M.; Park, J. W.; Sato, T.; Teramoto, A.; Lifson, S.; Selinger, R. L. B.; Selinger, J. V. *Angew. Chem., Int. Ed.* **1999**, *38*, 3138−3154.

(18) Green, M. M.; Reidy, M. P.; Johnson, R. D.; Darling, G.; O'Leary, D. J.; Willson, G. *J. Am. Chem. Soc.* **1989**, *111*, 6452−6454.

(19) Green, M. M.; Garetz, B. A.; Munoz, B.; Chang, H.; Hoke, S.; Cooks, R. G. *J. Am. Chem. Soc.* **1995**, *117*, 4181−4182.

(20) Green, M. M.; Andreola, C.; Munoz, B.; Reidy, M. P.; Zero, K. *J. Am. Chem. Soc.* **1988**, *110*, 4063−4065.

(21) Green, M. M.; Zanella, S.; Gu, H.; Sato, T.; Gottarelli, G.; Jha, S. K.; Spada, G. P.; Schoevaars, A. M.; Feringa, B. L.; Teramoto, A. *J. Am. Chem. Soc.* **1998**, *120*, 9810−9817.

(22) (a) Cheon, K. S.; Selinger, J. V.; Green, M. M. *Angew. Chem., Int. Ed.* **2000**, *39*, 1482−1485. (b) Tang, K.; Green, M. M.; Cheon, K. S.; Selinger, J. V.; Garetz, B. A. *J. Am. Chem. Soc.* **2003**, *125*, 7313−7323.

(23) For representative examples of other temperature-based helical-switching polymers, see: (a) Watanabe, J.; Okamoto, S.; Satoh, K.; Sakajiri, K.; Furuya, H.; Abe, A. *Macromolecules* **1996**, *29*, 7084−7088. (b) Maeda, K.; Okamoto, Y. *Macromolecules* **1998**, *31*, 5164−5166. (c) Fujiki, M. *J. Am. Chem. Soc.* **2000**, *122*, 3336−3343. (d) Zhao, H.; Sanda, F.; Masuda, T. *Macromolecules* **2004**, *37*, 8888−8892. (e) Maeda, K.; Mochizuki, H.; Watanabe, M.; Yashima, E. *J. Am. Chem. Soc.* **2006**, *128*, 7639−7650. (f) Hasegawa, T.; Morino, K.; Tanaka, Y.; Katagiri, H.; Furusho, Y.; Yashima, E. *Macromolecules* **2006**, *39*, 482−488.

(24) Maxein, G.; Zentel, R. *Macromolecules* **1995**, *28*, 8438−8440.

(25) The system is very sensitive to small structural changes, as well as variations in the amount of switch units on the polymer chain and its concentration, see: (a) Müller, M.; Zentel, R. *Macromolecules* **1996**, *29*, 1609−1617. (b) Mayer, S.; Maxein, G.; Zentel, R. *Macromolecules* **1998**, *31*, 8522−8525.

(26) Li, J.; Schuster, G. B.; Cheon, K. S.; Green, M. M.; Selinger, J. V. *J. Am. Chem. Soc.* **2000**, *122*, 2603−2612.

Scheme 1. Photochemical and Thermal Isomerization Steps for Chain-End Molecular Motor Functionalized **1**-PHIC (ref 6d)

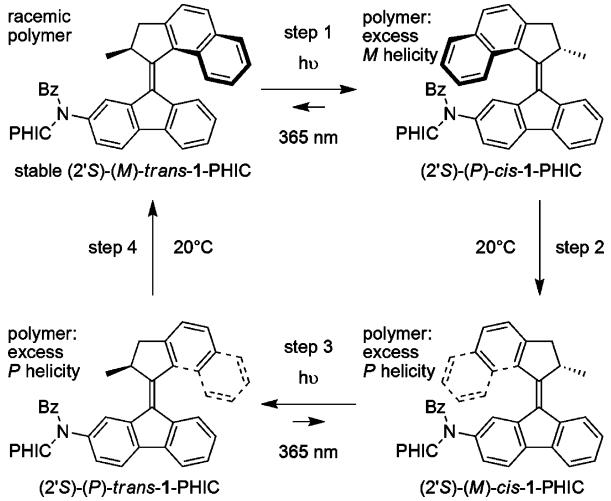

tributed along the polymer chain was transferred to the backbone of the polymer. Besides having a relatively small chiral influence toward the helical backbone, this also fundamentally changes the structure, and physical properties (e.g., solubility and aggregation behavior in the LC phase), of the polymer. Alternatively, incorporation of the switch unit at the terminus of the polymer leads to little change in the properties of the polymer, except for the chirality. Recently, we showed that effective chiral induction by a single chiral photochromic unit (a light-driven molecular motor), covalently attached at the terminus of a poly(*n*-hexyl isocyanate) (PHIC) (**1** in Scheme 1), allows fully reversible control over the preferred helical sense of the polymer backbone.[6d] A drawback of our original system is the fact that both light and heat are used as control elements to achieve the chiral induction toward the polymer. As temperature variation by itself, regardless of the switching aspects in this system, can have a large effect on the cholesteric state of a lyotropic LC, we anticipated that a system that is fully controllable with light at one set temperature would be particularly suitable to achieve precise control over the helicity of a cholesteric LC phase.

Herein, we show that the molecular chirality of the chiroptical switch can be transmitted, via the macromolecular level of the polyisocyanate, further to the supramolecular level of a cholesteric LC phase generated by these functionalized polymers (Figure 1). The current system is actually the first in which full control of the cholesteric handedness of the lyotropic LC phase is allowed with light. Furthermore, this is accomplished by simply modifying the end-group, inducing minimal change in the physical properties of the polymer, whereas in all previously developed systems in which a small cholesteric pitch alteration can be induced photochemically, multiple switches are appended.[16] Our system is also unique as the chirality of the switch unit gets completely inverted. To the best of our knowledge, our system is the first where the sign and magnitude of the chirality of the LC material can be completely switched by light using a single molecular switch in each lyotropic LC component.

Molecular Design

Unidirectional rotation with the molecular motor system attached at the polymer chain's terminus in the previously

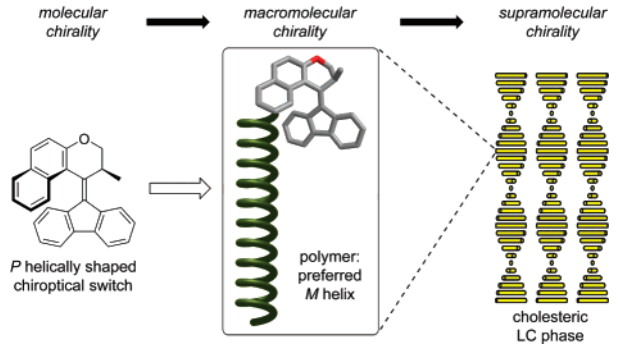

Figure 1. Schematic representation of the hierarchical transmission of chiral information from the molecular level of a single chiroptical switch molecule, via the macromolecular level of a polyisocyanate, to the supramolecular level of a cholesteric LC phase.

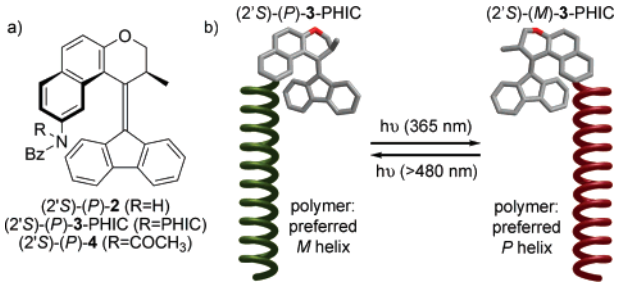

Figure 2. (a) Benzamide-functionalized chiroptical molecular switch **2**, chain-end chiroptical switch functionalized poly(*n*-hexyl isocyanate) **3**, and *N*-acylated chiroptical molecular switch **4** and (b) schematic representation of the reversible inversion of the preferred helical twist sense of a polymer backbone induced by a chiroptical molecular switch at its terminus. (2′*S*)-(*P*)-**3**-PHIC induces a preferred *M* helical twist of the polymer backbone. UV irradiation (λ = 365 nm) of the photochromic switch, yielding (2′*S*)-(*M*)-**3**-PHIC, leads to an induced preferred *P* helicity of the polymer. Subsequent irradiation with visible light (λ > 480 nm) reverts the system to (2′*S*)-(*P*)-**3**-PHIC with a preferred *M* helicity of the polymer.

reported system **1**-PHIC is achieved in a four-step switching cycle by a combination of two photochemically induced cis−trans isomerizations, each followed by an essentially irreversible and fast thermal isomerization (Scheme 1).[27] This makes control of the exact composition of the mixture of isomers and the associated chiral induction toward the polymer chain upon irradiation of **1**-PHIC at room temperature a highly complex process.

In order to obtain better control over the chiral induction toward the helical polymer, the photochromic unit attached at the polymer chain's terminus first was redesigned into a photochemically bistable chiroptical switch which has two thermally stable states (**3**-PHIC in Figure 2). By attaching the polymer chain to the upper-half of the molecule in **3**-PHIC (Figure 2a) instead of to the lower-half as was the case in **1**-PHIC, a symmetrical fluorenyl-based lower-half is obtained while positioning the polymer in the fjord region of the switch unit. As the two thermally stable isomers in the rotary cycle (Scheme 1), as well as the two unstable isomers, are now degenerate, this effectively reduces the number of possible isomers from four to only two. The molecular motor now operates as a chiroptical switch with two distinct states: (2′*S*)-(*P*)-**3**-PHIC is converted, after a photochemically induced cis−trans isomerization around the central olefinic bond, to (2′*S*)-(*M*)-**3**-PHIC, resulting in an inversion of the intrinsic helical

(27) The half-lives at 20 °C for the thermal isomerizations involved with second-generation light-driven molecular motor **1** are approximately 5 min.

Scheme 2. Retrosynthesis for **2**

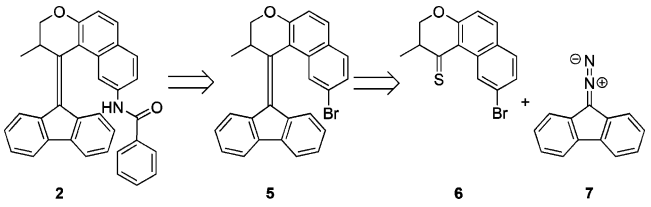

shape of the molecule from *P* to *M* (Figure 2b). In **3**-PHIC, one state induces a preferred *M* helicity, and the other induces a preferred *P* helicity of the polymer backbone. Moreover, using two different wavelengths, the two states of the chiroptical switch are addressable with light in a fully reversible manner.

The thermal helix inversion that follows the photochemical isomerization (step 2 and step 4 in Scheme 1), which involves the passage of both the naphthyl moiety and the methyl substituent in the upper-half of the molecule past the lower-half, reverts the molecule to the stable isomer with an intrinsic *P* helical shape. In order to obtain two thermally stable states and create a system that is fully photoaddressable, this thermal helix inversion step needs to be blocked. Therefore, the five-membered ring in the upper-half of the motor molecule connected to the central double bond in **1**-PHIC was changed to a six-membered ring in **3**-PHIC. It was reasoned that in **3**-PHIC, the naphthyl moiety in the upper-half of the molecule is pushed toward the lower-half, hampering the passage of this group along the planar and rigid fluorenyl-based lower part during the thermal helix inversion step, resulting in a strongly increased energy barrier for this thermal isomerization. The presence of the amide substituent at a position on the naphthalene in the upper-half of the molecule where it points toward the lower-half probably raises this energy barrier even further. The photochemically induced isomer can, however, be converted back to the original isomer (2′*S*)-(*P*)-**3**-PHIC by irradiation with visible (λ > 480 nm) light, as at these wavelengths only (2′*S*)-(*M*)-**3**-PHIC absorbs (vide infra).

As a result of these changes in design, **3**-PHIC can be switched between two states that are fully photoaddressable and thermally stable (Figure 2b). (2′*S*)-(*P*)-**3**-PHIC is anticipated to induce a preferred *M* helical twist sense of the polymer backbone, as the fluorenyl moiety of the lower-half of the molecule resides at one specific side of the polymer chain.[28] In (2′*S*)-(*M*)-**3**-PHIC, the fluorenyl-based lower-half is present at the other side of the polymer chain, which therefore should induce a preferred *P* helical twist sense of the polymer backbone.

Synthesis

The most important step in the synthetic route toward the envisioned chiroptical switch **2**, bearing a benzamide functionality to be used as an initiator of the *n*-hexyl isocyanate polymerization, is the formation of the sterically overcrowded central olefinic bond by coupling the two halves of the molecule via a Staudinger-type diazo-thioketone reaction[29] (Scheme 2). To avoid problems with the amide functionality arising from the harsh conditions involved with the synthesis of the upper-half thioketone precursor, the benzamide functionality was introduced in the last step of the synthesis via well-precedented palladium-catalyzed amidation conditions developed by Yin and Buchwald.[30]

Scheme 3. Synthesis of Upper-Half Ketone Precursor **13**

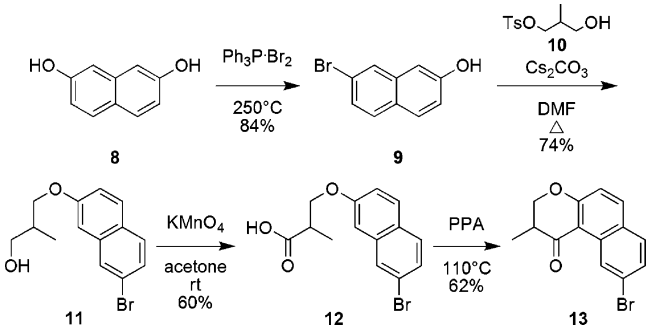

Scheme 4. Synthesis of Benzamide-Functionalized Chiroptical Switch **2** (xantphos = 4,5-Bis(diphenylphosphino)-9,9-dimethylxanthene)

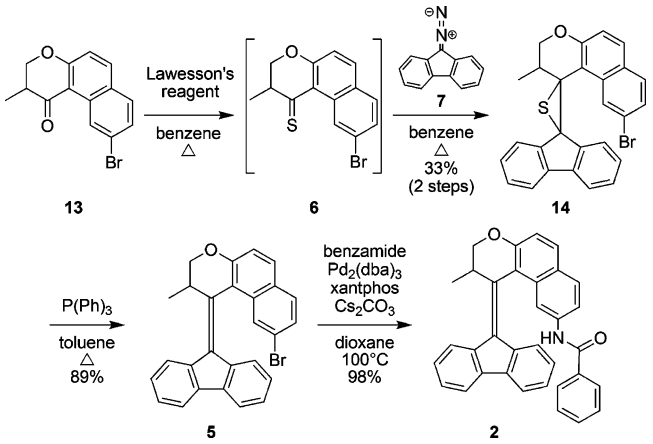

Synthesis of ketone precursor **13** was feasible in four steps (Scheme 3). First, 2,7-naphthalenediol **8** was transformed into 7-bromo-naphthalen-2-ol **9** by treatment with $PPh_3{\cdot}Br_2$ at elevated temperature following a literature procedure.[31] Subsequently, alkylation using tosylate **10** in refluxing DMF yielded compound **11** which, by the oxidation of the terminal primary alcohol, was converted to acid **12**. Regioselective ring-closure of the acid was achieved in polyphosphoric acid at elevated temperatures, yielding ketone **13**.

After the conversion of ketone **13** to the corresponding thioketone **6** by treatment with Lawesson's reagent, the diazo-thioketone coupling using diazofluorenone **7** provided episulfide **14** in 33% yield over the two steps (Scheme 4). Thioketone **6** proved to be rather unstable and was used immediately after a quick purification by flash column chromatography. Desulfurization of **14** by triphenylphosphine yielded alkene **5**, which was then used in the palladium-catalyzed amidation reaction[30] to introduce the benzamide functionality. Enantioresolution of **2** was achieved by CSP-HPLC (Chiralpak OD, heptane/2-propanol = 95:5).

Photochemistry of Benzamide-Functionalized Chiroptical Switch 2

The photoisomerizations of **2** (Scheme 5) were studied using UV−vis,[32] circular dichroism (CD) (Figure 3), and ^{1}H NMR

(28) In (2′*S*)-(*P*)-*cis*-**1**-PHIC, which also induces a preferred *M* helical twist sense of the polymer backbone, the upper-half of the motor molecule resides on the same side of the polymer chain as the fluorenyl-based lower-half of the chiroptical switch in the present system.

(29) (a) Barton, D. H. R.; Willis, B. J. *J. Chem. Soc., Chem. Commun.* **1970**, 1225−1226. (b) Buter, J.; Wassenaar, S.; Kellogg, R. M. *J. Org. Chem.* **1972**, *37*, 4045−4060.

Scheme 5. Photoisomerizations of Benzamide-Functionalized Chiroptical Switch **2**

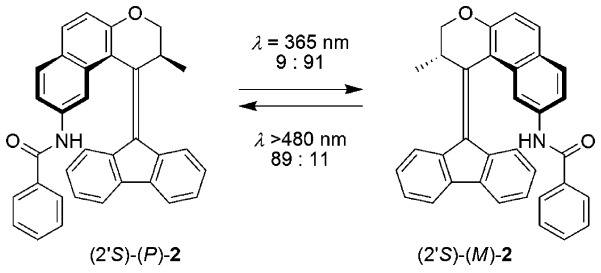

(Figure 4) spectroscopy. Irradiation of a sample of (2′*S*)-(*P*)-**2**[33] in Et_2O at 20 °C ($\lambda = 365$ nm) resulted in the appearance of a distinct absorption band around 450 nm in the UV−vis spectrum and a change in sign of the CD absorptions, indicative for the helix inversion of the molecule to provide diastereoisomer (2′*S*)-(*M*)-**2**. Upon irradiation ($\lambda = 365$ nm) of a sample of a racemic mixture of (2′*S**)-(*P**)-**2**[34] in CD_2Cl_2 for 3 h at 20 °C, new signals corresponding to the newly formed isomer (2′*S**)-(*M**)-**2** appeared in the ^{1}H NMR spectrum (Figure 4). The signal of the methyl substituent, a doublet at 1.42 ppm for (2′*S**)-(*P**)-**2**, shifts downfield to 1.58 ppm for (2′*S**)-(*M**)-**2**. Using HPLC analysis, a ratio of (2′*S*)-(*P*)-**2** to (2′*S*)-(*M*)-**2** of 9:91 at the photostationary state (PSS) of this photoequilibrium was determined.

Subsequent irradiation of the samples containing the PSS mixture with visible light ($\lambda > 480$ nm) lead to a near complete reversal of the changes in the UV−vis, CD, and ^{1}H NMR spectra, as at these wavelengths the extinction coefficient of (2′*S*)-(*M*)-**2** is much higher than that of (2′*S*)-(*P*)-**2** (Figure 3a), leading to the efficient conversion back to (2′*S*)-(*P*)-**2**. The PSS ratio of (2′*S*)-(*P*)-**2** to (2′*S*)-(*M*)-**2** of this photoequilibrium, as determined by HPLC analysis, was 89:11, indicating that efficient and selective switching in two directions is indeed possible with this system.

The geometry of the two isomers was unequivocally determined by X-ray analysis of the racemates (Figure 5). A solution of racemic (2′*S**)-(*P**)-**2** in CH_2Cl_2 was irradiated ($\lambda = 365$ nm) for 5 h. Thereafter, via slow evaporation under *n*-pentane atmosphere, crystals suitable for X-ray analysis, containing both (2′*S**)-(*P**)-**2** and (2′*S**)-(*M**)-**2**, were obtained. In the (2′*S**)-(*P**)-**2** isomer, the upper heterocyclic ring adopts the twisted boat conformation (Figure 5a) which was observed before with structurally analogous chiroptical switches and molecular motors.[10a,11c] The methyl substituent adopts a pseudoaxial orientation, which allows it to point away from the lower-half of the molecule, in the same direction as the naphthyl group does. With the previously described systems,[10a,11c] the twisted boat conformation of the six-membered ring in the upper-half is inverted in the isomer obtained after the photochemically induced cis−trans isomerization. With the molecular motors this forces the methyl substituent in a pseudoequatorial orientation, in close proximity to the lower-half of the molecule and residing on the same side of this lower-half as the naphthyl moiety. In the case of photochemically generated isomer (2′*S**)-(*M**)-**2** (Figure 5b), the twisted boat conformation of this six-membered ring in the upper-half is not inverted with respect to the conformation in (2′*S**)-(*P**)-**2**. The methyl substituent retains a pseudoaxial orientation, yet it ends up at the other face of the fluorenyl-based lower-half with respect to the substituted naphthyl moiety, resulting in the twisted structure shown.

In order to observe the reversal of the spectral changes, corresponding to the conversion of (2′*S*)-(*M*)-**2** to (2′*S*)-(*P*)-**2** via the thermal helix inversion process, heating to at least 80 °C was required. The kinetics and thermodynamic parameters of this thermal helix inversion were determined by monitoring the UV signal at 470 nm over time in the dark at five different temperatures ranging from 80 to 100 °C. Using the various rate constants, the Gibbs free energy of activation was calculated using the Eyring equation: $\Delta^{\ddagger}G^{\circ} = 112.9$ kJ·mol^{-1} ($\Delta^{\ddagger}H^{\circ} = 112.0$ kJ·mol^{-1}, $\Delta^{\ddagger}S^{\circ} = -3.0$ J·mol^{-1}·K^{-1}).[32] By extrapolation of the kinetic data, a half-life of (2′*S*)-(*P*)-**2** at 20 °C of 459 days was determined ($k = 1.75 \times 10^{-8}$ s^{-1}), indicating that for the irradiation experiments using the switchable LC film at room temperature (vide infra) this thermal step is effectively blocked.

Polymerization

The polymerization of *n*-hexyl isocyanate (HIC) was accomplished via a slightly altered version of the procedure developed by Ahn et al.[35] After the addition of NaH to a solution of enantiomerically pure (2′*S*)-(*P*)-**2** in THF at room temperature, the mixture was cooled to −90 °C and 100 equiv of the monomer (HIC) was added (Scheme 6). After 45 min, acetyl chloride and pyridine were added to end-cap the polymers. Precipitation of the polymer from MeOH afforded the polymer in 71% yield. Analysis by GPC ($M_w = 32\,650$)[36] and ^{1}H NMR[37] spectroscopy indicated an average degree of polymerization of approximately 200. Acetylation of (2′*S*)-(*P*)-**2** afforded switch molecule (2′*S*)-(*P*)-**4** (Scheme 6), which was used as a CD reference compound: the CD spectra of the different isomers of **4** allowed us to discriminate between the CD absorptions of the helical polymer and that of the chiroptical switch molecule connected to it.

Photochemistry of Chiroptical Switch Functionalized Polyisocyanate 3

The photoisomerizations of **3**-PHIC were followed by CD spectroscopy, using the CD spectra of the different isomers of **4** to distinguish between the CD contributions of the helical polymer and those of the chiroptical molecular switch connected to it (Figure 6). The spectra of the polymer and the acetylated switch completely overlap between 300 and 500 nm. In this wavelength region, polyisocyanate does not absorb and the CD signals of the polymer−switch hybrid originate solely from the attached switch molecule. Between 210 and 280 nm a strong deviation of the CD curve of **3**-PHIC from the CD curve of acetylated switch **4** was observed (Figure 6a), and subtraction

(30) Yin, J. J.; Buchwald, S. L. *Org. Lett.* **2000**, *2*, 1101−1104.
(31) Lustenberger, P.; Diederich, F. *Helv. Chim. Acta* **2000**, *83*, 2865−2883.
(32) See the Supporting Information for details.
(33) Assignment of the absolute configuration was done by comparison with CD data of related compounds (see refs 11b and 11c).
(34) The asterisks indicate the fact that a racemic mixture of (2′*S*)-(*P*)-**2** and (2′*R*)-(*M*)-**2** was used; the absolute configuration and helicity of one of the enantiomers is given here for clarity.
(35) Ahn, J.-H.; Shin, Y.-D.; Nath, G. Y.; Park, S.-Y.; Rahman, M. S.; Samal, S.; Lee, J.-S. *J. Am. Chem. Soc.* **2005**, *127*, 4132−4133.
(36) As the GPC columns were calibrated using standard solutions of polystyrene, a polymer with a hydrodynamic volume differing from that of polyisocyanate, the value obtained with this technique is not very accurate and can only be used as an indication.
(37) By comparing the integrals of the signals of the C_6H_{13} side chains in every monomeric unit and the signals of the aromatic protons of the photochromic unit at the polymer's terminus in the ^{1}H NMR spectrum, an estimate of the chain length can be made.

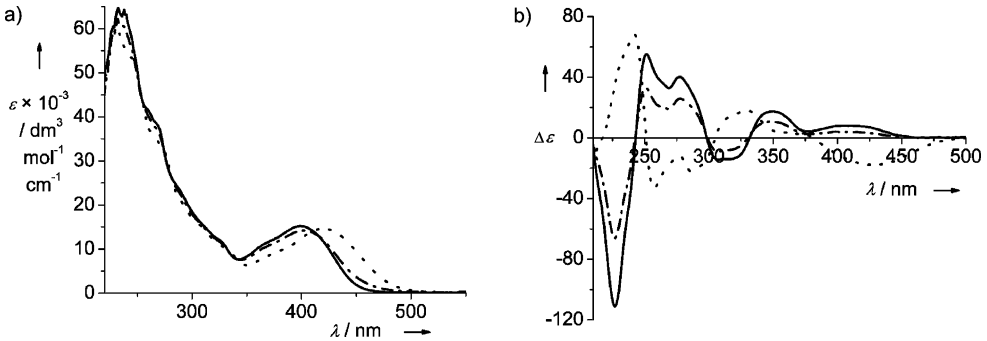

Figure 3. UV−vis (a) and CD (b) spectra (Et_2O, 20 °C) of (2′*S*)-(*P*)-**2** (solid line), the PSS mixture with (2′*S*)-(*P*)-**2** and (2′*S*)-(*M*)-**2** (dotted line) after UV irradiation (λ = 365 nm), and the PSS mixture of (2′*S*)-(*P*)-**2** and (2′*S*)-(*M*)-**2** (dashed line) after irradiation with visible light (λ > 480 nm).

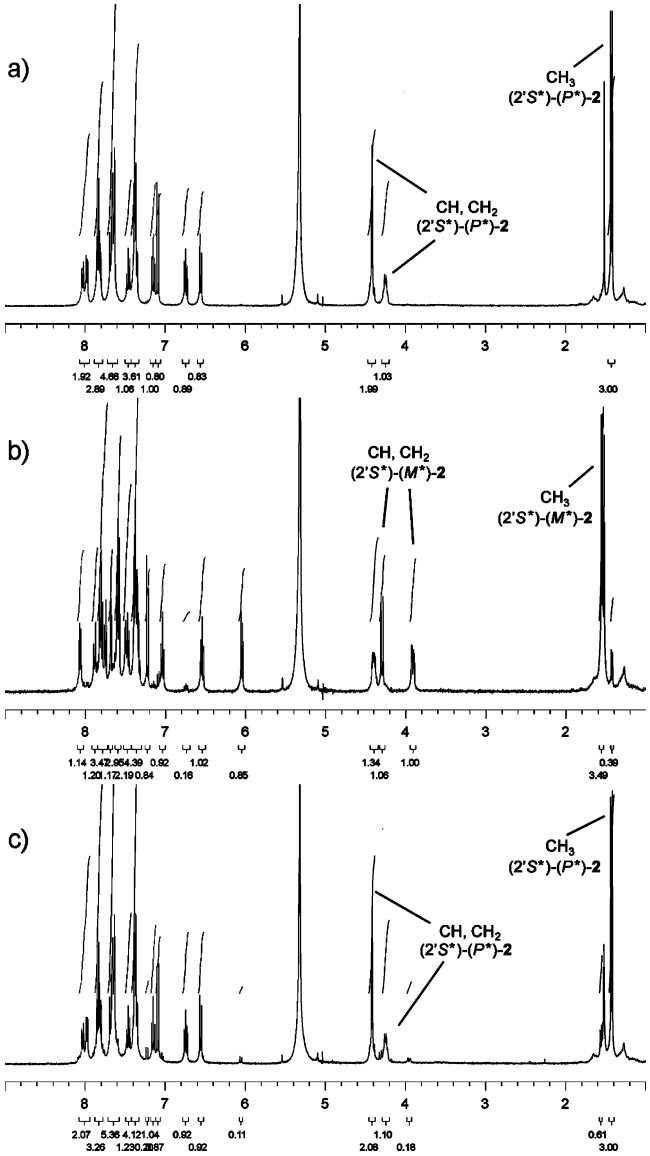

Figure 4. ^{1}H NMR (20 °C, CD_2Cl_2) of (a) (2′*S**)-(*P**)-**2** before irradiation, (b) the PSS mixture of (2′*S**)-(*P**)-**2** and (2′*S**)-(*M**)-**2** after UV irradiation (λ = 365 nm), and (c) the PSS mixture of (2′*S**)-(*P**)-**2** and (2′*S**)-(*M**)-**2** after irradiation with visible light (λ > 480 nm).

of the CD spectrum of (2′*S*)-(*P*)-**4** from the CD spectrum of (2′*S*)-(*P*)-**3**-PHIC yielded a CD difference spectrum typical of PHIC with an excess of the *M* (left-handed) helical sense of the backbone (solid line in Figure 6d). Interestingly, a 3-fold increase in intensity of the molar elipticity (Figure 6d), compared

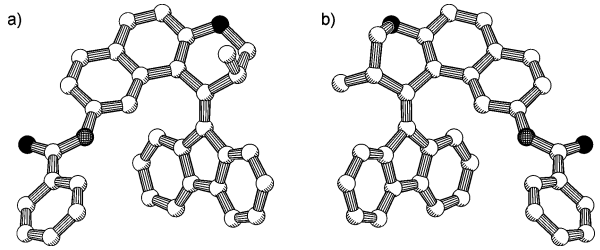

Figure 5. Pluto drawings of (a) (2′*S**)-(*P**)-**2** and (b) (2′*S**)-(*M**)-**2**. One enantiomer is shown for both isomers; this structure does not express the absolute stereochemistry of the molecule.

Scheme 6. Anionic Polymerization of *n*-Hexyl Isocyanate Using the Sodium Salt of Benzamide-Functionalized Chiroptical Switch **2** as the Initiator (Top), and Acetylation of the Amide Yielding Chiroptical Switch **4** (Bottom)

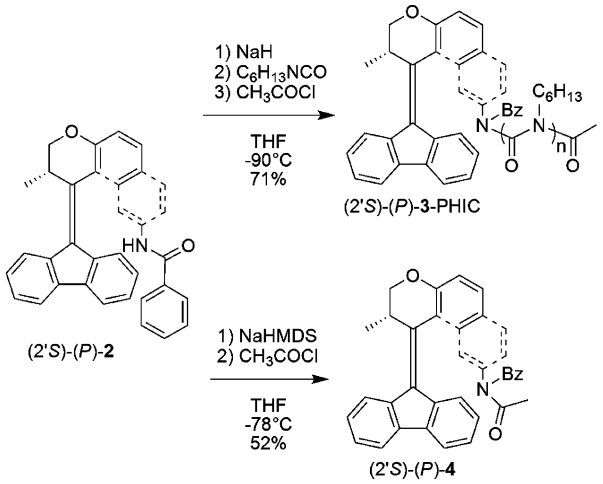

to that obtained with the previously described system **1**,[6d] was found. Apparently, the chiral induction from the chiroptical switch to the polymer chain is significantly increased in **3**-PHIC compared to **1**, which is attributed to a more pronounced influence of the molecular helix structure of the switching unit at this new position of attachment (in the fjord region) to the photochromic molecule. We reason that this effect is also caused by the fact that the five-membered ring in the upper-half of the motor molecule connected to the central double bond in **1** has expanded to a six-membered ring in **3** by introduction of the oxygen atom. Together with the naphthyl moiety in the upper-half, the polymer chain is thereby "pushed" closer to the fluorenyl-based lower-half of the molecule, leading to the enhanced chiral induction.

Upon irradiation of a sample of (2′*S*)-(*P*)-**3**-PHIC in Et_2O at 20 °C with UV light (λ = 365 nm), providing (2′*S*)-(*M*)-**3**-

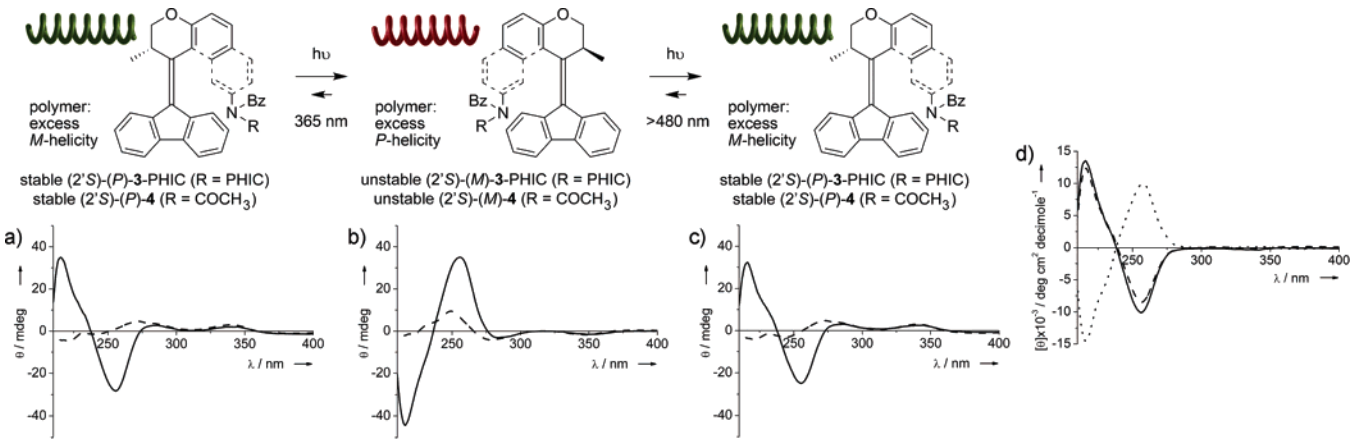

Figure 6. CD spectra (Et_2O, 20 °C) of (a) (2′*S*)-(*P*)-**3**-PHIC (38.3 mg/L) (solid) and (2′*S*)-(*P*)-**4** (3.2 μM) (dashed), (b) the PSS mixture with (2′*S*)-(*P*)-**3**-PHIC and (2′*S*)-(*M*)-**3**-PHIC (solid) and the PSS mixture with (2′*S*)-(*P*)-**4** and (2′*S*)-(*M*)-**4** (dashed) after UV irradiation (λ = 365 nm), (c) the PSS mixture of (2′*S*)-(*M*)-**3**-PHIC and (2′*S*)-(*P*)-**3**-PHIC (solid) and the PSS mixture of (2′*S*)-(*M*)-**4** and (2′*S*)-(*P*)-**4** (dashed) after irradiation with visible light (λ > 480 nm), and (d) molar ellipticity of the polymer backbone (CD difference spectra polymer **3** − acetylated switch **4**) for the stable (2′*S*)-(*P*)-isomer of the chiroptical switch (solid), after UV irradiation (λ = 365 nm) (dotted), and after irradiation with visible light (λ > 480 nm) (dashed).

PHIC,[38] the prominent absorption maxima around 220 and 260 nm in the CD spectrum inverted (Figure 6b). Irradiation of a sample of (2′*S*)-(*P*)-**4** under the same conditions resulted in an inversion of the CD absorptions in accordance with the inversion of the intrinsic chirality of the molecule to provide (2′*S*)-(*M*)-**4**. Most obvious is the inversion of the CD difference spectrum (solid vs dotted line in Figure 6d), indicating that the polymer backbone has switched from a predominant *M* to *P* helical sense.

Subsequent irradiation of the sample containing (2′*S*)-(*M*)-**3**-PHIC with visible light (λ > 480 nm), providing (2′*S*)-(*P*)-**3**-PHIC,[39] resulted again in an inversion of the prominent CD signals of the polymer (Figure 6c). Irradiation under the same conditions of a sample containing (2′*S*)-(*M*)-**4** resulted also in an inversion of the CD absorptions, again in accordance with the inversion of the intrinsic helicity of the acetylated switch to provide (2′*S*)-(*P*)-**4**. The inverted CD signals of the polymer, again clearest observed from the CD difference spectrum (dashed line in Figure 6d), indicate that the polymer backbone has switched back to a preferred *M* helical twist sense. The CD spectrum does not return completely to the spectrum obtained before the irradiation experiments, as a PSS mixture still containing a small amount of (2′*S*)-(*M*)-**3**-PHIC is obtained.

Photochemistry of the LC Matrix

The effect of the photoinduced inversion of the predominant helicity of the polymer, on a lyotropic cholesteric liquid crystalline phase generated by these polymers, was subsequently investigated.[40] A 30 wt % solution of (2′*S*)-(*P*)-**3**-PHIC in toluene was placed between two flat KBr plates in a liquid IR cell, in which the layer thickness of 200 μm was controlled using a Teflon spacer. The LC was allowed to organize and orient for a period of 16 h, after which it was analyzed using an optical microscope equipped with crossed polarizers. Initially, a polygonal fingerprint texture was observed (Figure 7a), which is typical for a cholesteric LC phase with an alignment of the cholesteric helix axis parallel to the surface.[41] The periodicity of the polygonal texture corresponds to half a pitch length, which was used to determine a pitch length of 6.0 μm.[42] The sample was then followed in time at a fixed location throughout the irradiation experiments. Upon UV irradiation (λ = 365 nm), leading to the conversion of (2′*S*)-(*P*)-**3**-PHIC, a polymer with a preferred *M* helical twist sense, to (2′*S*)-(*M*)-**3**-PHIC with preferred *P* helicity, the distance between the lines of the polygonal texture clearly increased, indicating an elongation of the cholesteric helical pitch of the LC. Initially, only a slight increase in the line distance in the fingerprint texture was observed, as after 15 min of irradiation a pitch length of 6.2 μm was determined (Figure 7b). After 45 min, the distance between the lines had increased much further, and the lines slowly started to fade out until almost no fingerprint texture was observed anymore (Figure 7c). At this point the pitch has elongated to such an extent that the cholesteric lines are no longer detectable by eye. Upon further UV irradiation the fingerprint texture redeveloped, indicating a shortening of the pitch length. Interestingly, during this process, initially circular patterns were observed (Figure 7d, after 90 min of UV irradiation).[43] During continual irradiation, the circular patterns slowly merged (Figure 7e), generating more homogeneous areas of the polygonal fingerprint texture. The UV irradiation was stopped after 150 min, as no changes in the polygonal fingerprint texture seemed to occur anymore. However, a fully homogeneous fingerprint texture, similar to that observed before the irradiation experiment, was observed after the sample had been left in the dark overnight. At this point, a pitch length of 4.5

(38) A PSS mixture of (2′*S*)-(*P*)-**3**-PHIC and (2′*S*)-(*M*)-**3**-PHIC is obtained. For **2** a PSS ratio of (2′*S*-(*P*)-**2**/(2′*S*)-(*M*)-**2** = 9:91 was determined; for **3** a similar PSS is anticipated.

(39) A PSS mixture of (2′*S*)-(*P*)-**3**-PHIC and (2′*S*)-(*M*)-**3**-PHIC is obtained. For **2** a PSS ratio of (2′*S*-(*P*)-**2**/(2′*S*)-(*M*)-**2** = 89:11 was determined; for **3** a similar PSS is anticipated.

(40) After the addition of (2′*S*)-(*P*)-**2** as a chiral dopant to an LC film of unfunctionalized PHIC (formed by initiation of the polymerization with benzanilide, see ref 35) in toluene, the LC remained nematic. Apparently, the intermolecular interactions of the switch with the polymers alone are not sufficient to induce a nematic-to-cholesteric phase transition of the LC matrix.

(41) A 520 nm cutoff filter was placed between the light source of the microscope and the sample, in order to prevent any photoconversion to be caused by this light source. For this reason the pictures of the UV irradiation series (Figure 7) are slightly darker compared to the pictures of the visible light irradiation series (Figure 8).

(42) The cholesteric pitch length of the sample was determined from the periodicity of the fingerprint texture. The values presented are an average of three measurements per optical micrograph. The average deviation is always within 5%.

(43) The circular patterns that emerge initially during the re-formation of the fingerprint texture (Figure 7, parts d and e) have been observed previously with other cholesteric LC materials: Bouligand, Y. *J. Phys.* **1973**, *34*, 603−614.

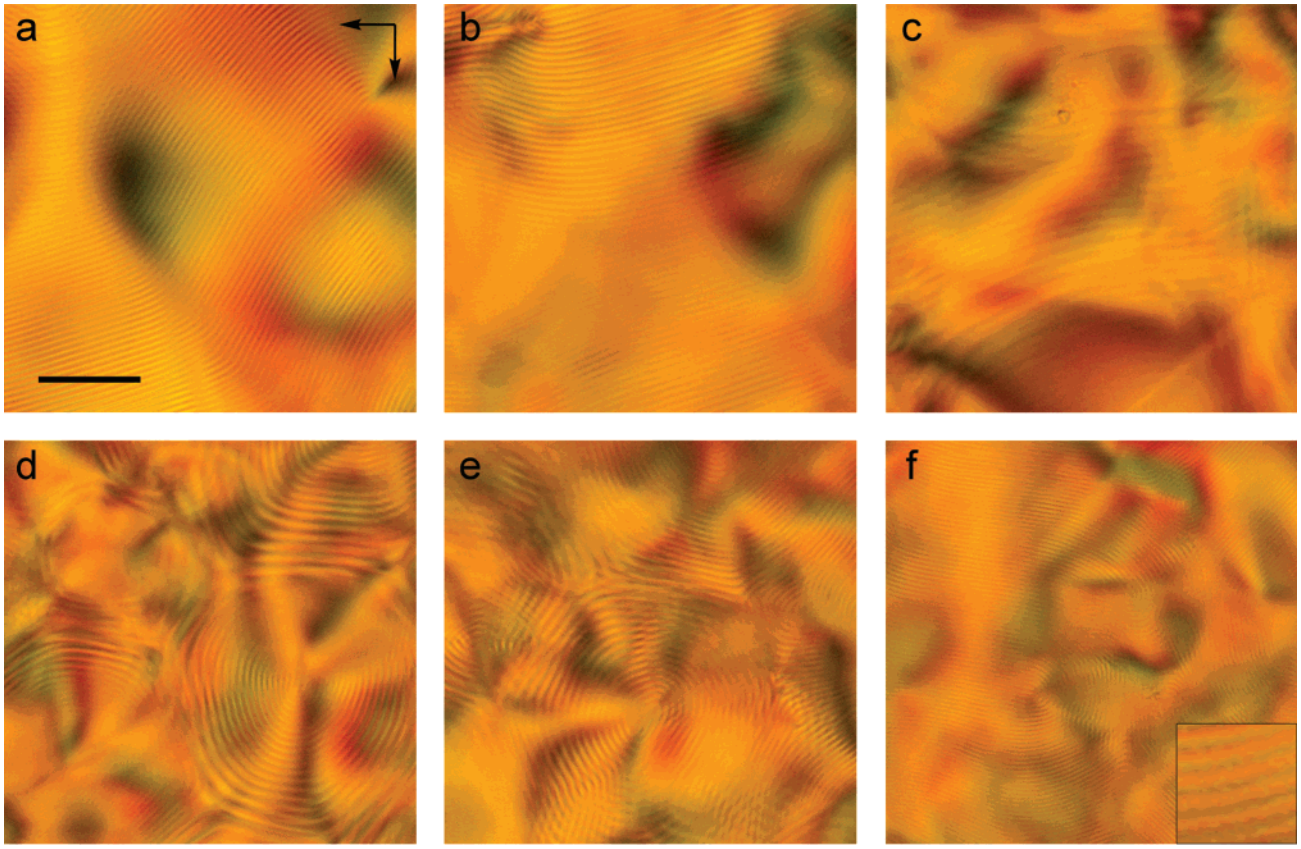

Figure 7. Optical micrographs of a thin film (thickness, 200 μm) of (2′*S*)-(*P*)-**3**-PHIC in toluene (30 wt %) (a) before irradiation ($p = 6.0$ μm), (b) after 15 min ($p = 6.2$ μm), (c) 45 min, (d) 90 min, and (e) 150 min of UV irradiation ($\lambda = 365$ nm), after which a PSS mixture is obtained that consists of a large excess of (2′*S*)-(*M*)-**3**-PHIC over (2′*S*)-(*P*)-**3**-PHIC, and (f) after leaving the irradiated sample in the dark overnight ($p = 4.5$ μm) (the inset shows an enlarged section under 5× higher magnification). Scale bar, 50 μm. The arrows indicate the directions of the crossed polarizers.

μm was determined, which is shorter than the pitch of 6.0 μm observed before the irradiation experiment (Figure 7, part f vs part a).

Subsequent irradiation of the sample with visible light ($\lambda >$ 480 nm), leading to the conversion of (2′*S*)-(*M*)-**3**-PHIC, a polymer with a preferred *P* helical twist sense, to (2′*S*)-(*P*)-**3**-PHIC with preferred *M* helicity of the polymer, resulted again in an increase in the distance between the lines in the polygonal texture, indicating an increase in the cholesteric pitch length. After 5 h of irradiation, an increase to 7.8 μm was determined (Figure 8a).[44] Continuing irradiation of the phase led to a further elongation of the pitch (13 μm after 6 h, see Figure 8b) and eventually a disappearance of the cholesteric lines (Figure 8c). The fingerprint texture reappeared upon further visible light irradiation, and the distance between the lines slowly decreased with time, indicating a shortening of the pitch length from approximately 22 μm[45] after 8 h (Figure 8d) to 9.0 μm after 9 h (Figure 8e). After 24 h of visible light irradiation, the fingerprint texture of the LC phase ceased to change, at which point a pitch length of 3.7 μm was reached (Figure 8f), again remarkably shorter than the 6.0 μm pitch observed before the irradiation experiments. The irradiation cycles of the liquid crystalline system are reversible and can be repeated several times.

Initially the sample contains solely (2′*S*)-(*P*)-**3**-PHIC, a polymer with a preferred *M* helical twist sense, leading to a *P* helical cholesteric LC phase[46] with a tight pitch (Figures 7a and 9a). Upon UV irradiation ($\lambda = 365$ nm), (2′*S*)-(*P*)-**3**-PHIC is converted to (2′*S*)-(*M*)-**3**-PHIC with a preferred *P* helical twist sense, which induces a cholesteric LC phase with the opposite helicity (*M*). This results in the observed elongation of the cholesteric pitch length upon UV irradiation (Figures 7b and 9b). At a certain point, equal amounts of *M* and *P* helical polymer are present in the LC film, effectively canceling each other's helical induction toward the cholesteric LC. This results in a near-infinite pitch length, and a sample that appears to be nematic, explaining the observed disappearance of the cholesteric texture (Figures 7c and 9c). Further irradiation leads to an excess (2′*S*)-(*M*)-**3**-PHIC over (2′*S*)-(*P*)-**3**-PHIC, resulting in a shortening of the pitch length of the cholesteric phase, which has now the *M* helicity, observed as the reappearance of the fingerprint texture (Figure 7, parts d and e, and Figure 9d). Continuous UV irradiation gradually increases the (2′*S*)-(*M*)-**3**-PHIC to (2′*S*)-(*P*)-**3**-PHIC ratio, explaining the observed shortening of the periodicity of the cholesteric corrugation, until the PSS is reached (Figures 7f and 9e). Subsequent irradiation with visible light ($\lambda >$ 480 nm) leads to the conversion of (2′*S*)-(*M*)-**3**-PHIC back to (2′*S*)-(*P*)-**3**-PHIC. This results in the

(44) Owing to the lower intensity of the light source used for the visible light irradiation compared to the UV irradiation, longer irradiation times are needed here in order to obtain the same changes of the LC phase.

(45) The value given for the pitch here is only approximate, due to the inhomogeneity of the periodicity in this micrograph.

(46) A rationalization of the relationship between the twist sense of the polyisocyanate and the handedness of the cholesteric LC formed by these polymers can be found in ref 21.

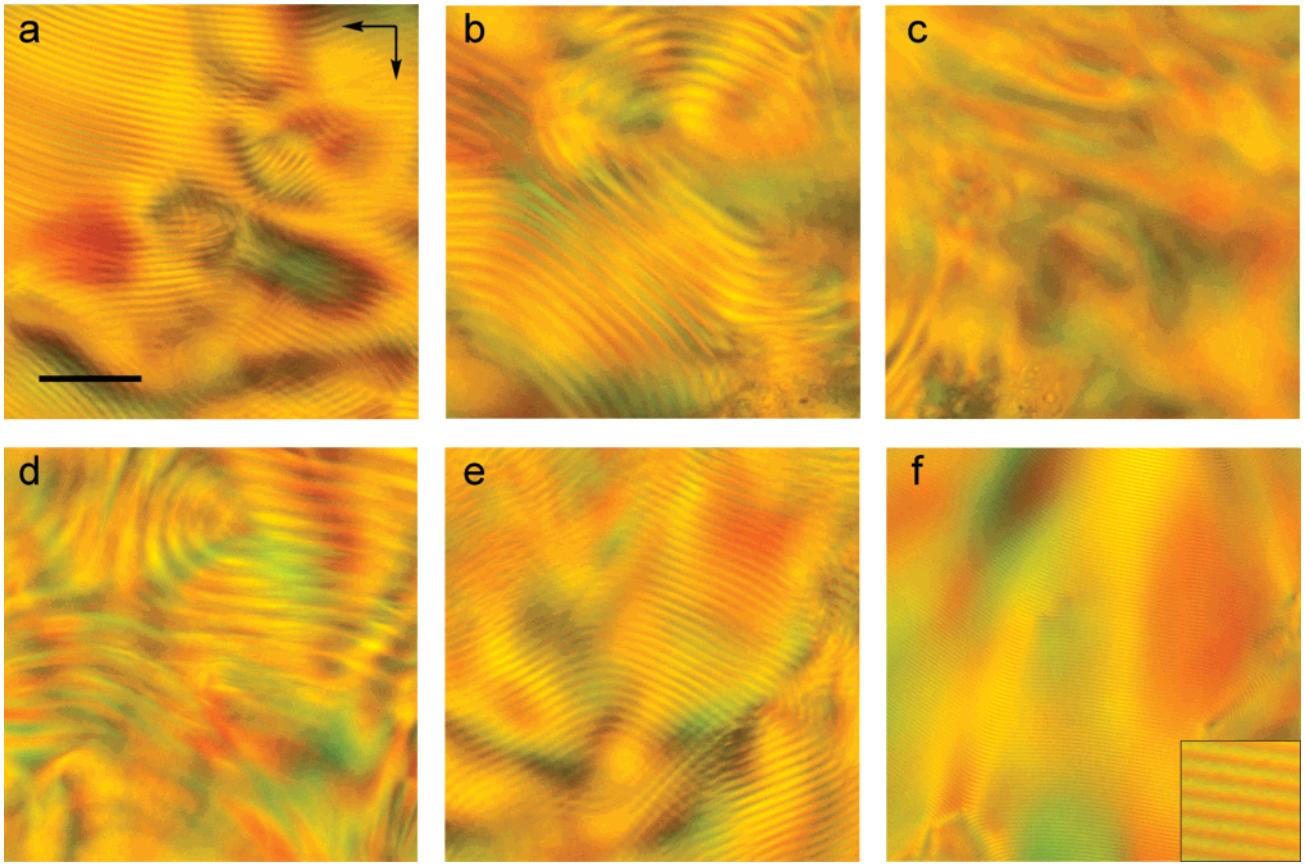

Figure 8. Optical micrographs of a thin film (thickness, 200 μm) of the PSS mixture obtained upon UV irradiation that consists of a large excess of (2′*S*)-(*M*)-**3**-PHIC over (2′*S*)-(*P*)-**3**-PHIC in toluene (30 wt %), after (a) 5 h ($p = 7.8$ μm), (b) 6 h ($p = 13$ μm), (c) 7 h, (d) 8 h ($p = 22$ μm), (e) 10 h ($p = 9.0$ μm), and (f) 24 h of irradiation with visible light ($\lambda > 480$ nm), after which a PSS mixture is obtained that consists of a large excess of (2′*S*)-(*P*)-**3**-PHIC over (2′*S*)-(*M*)-**3**-PHIC ($p = 3.7$ μm) (the inset shows an enlarged section under 5× higher magnification). Scale bar, 50 μm. The arrows indicate the directions of the crossed polarizers.

reversal of the changes of the cholesteric LC phase and a repetition of the observations that were described before (Figures 8 and 9).

Discussion and Conclusions

We have demonstrated that irradiation with light of different wavelengths allows fully reversible control over sign and magnitude of the cholesteric helical pitch of the LC phase of (2′*S*)-(*P*)-**3**-PHIC. The thermal reorganization observed for the UV irradiated sample after it had been stored in the dark overnight (Figure 7, part e vs part f) implies that the reorganization of the LC is slow[47] compared to the photoisomerization of the chiroptical switch−polymer hybrid.[48] As the photoisomerization upon visible light irradiation (the reverse process) takes place on a much longer time scale compared to the UV irradiation experiment, caused by the fact that a light source of much lower intensity was used, this thermal reorganization process was not observed after terminating the visible light irradiation. In this case, the photoisomerization and the thermal reorganization of the LC phase appear to take place on the same time scale.[49]

A puzzling observation is the fact that the pitch length of the cholesteric phase at both PSSs (4.5 μm at PSS_{365}, Figure 7f, and 3.7 μm at $PSS_{>480}$, Figure 8f) are substantially shorter than the pitch length of the nonirradiated sample (6.0 μm, Figure 7a). A slight reduction of the pitch has also been observed after irradiation of an LC based on an azobenzene-functionalized helical polymer and was attributed to solvent evaporation due to heating of the sample under the UV lamp, leading to a change in concentration.[16d] Upon increasing the concentration of (2′*S*)-(*P*)-**3**-PHIC in the lyotropic LC phase from 30 to 40 wt % indeed a decrease in pitch length from 6.0 to 2.9 μm was observed.[32] To verify if this could provide an explanation for the observed effect, a sample of (2′*S*)-(*P*)-**3**-PHIC in toluene was submitted to a number of irradiation cycles, in which first 1 h of UV irradiation was applied resulting in an increase in pitch length of the LC sample to almost nematic, after which it was irradiated 20 h with visible light. The initial pitch length of the sample, before irradiation was applied, was 6.9 μm.[50] After the first irradiation cycle, the pitch had decreased to a value of 4.4 μm,[32] a similar decrease in pitch length over one

(47) An apparent deficiency of this switchable system, in view of its potential applicability, appears to be the slow reorganization of the LC, a feature that seems to be common for any switching system based on a lyotropic LC, see, e.g., refs 9a, 16, and 22b. However, it has been observed that switching of the temperature responsive lyotropic LC described in ref 22b, when the temperature-based helicity-switching polymer was applied as the mesogen, followed the temperature change immediately.

(48) Switching of the photochromic unit, when an appropriate light source is used, takes place on the time scale of picoseconds.

(49) A slower reorganization would render a lyotropic LC system inferior to switchable thermotropic LCs, where the reorganization of the LC phase generally follows the switching of the dopant directly. However, the long irradiation times needed in the current experiments can be attributed to the experimental setup and relatively weak light sources used. Furthermore, lyotropic LCs have an important advantage over thermotropic LCs, in that there is no temperature-dependent phase boundary in these systems, as stated in ref 22b.

(50) This is somewhat longer than the 6.0 μm observed with the previous unirradiated sample. We assume this is caused by a slightly lower concentration of this particular sample.

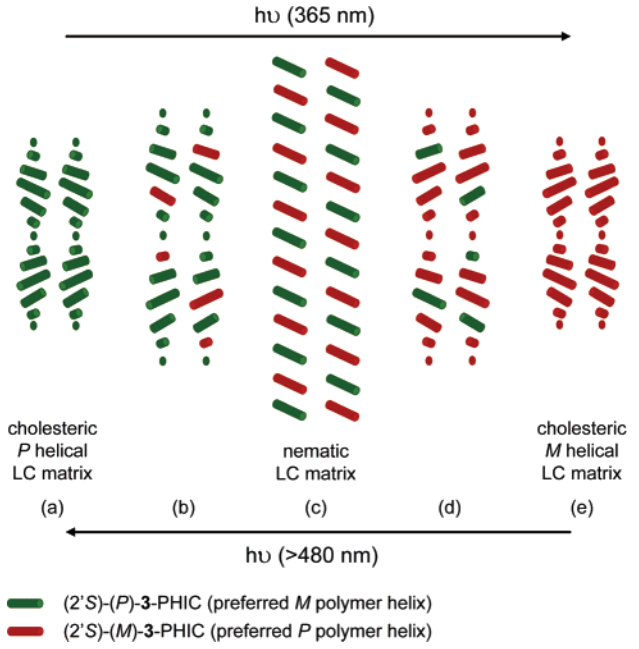

Figure 9. Schematic representation of the full photocontrol of the magnitude and sign of the supramolecular helical pitch of a cholesteric LC phase generated by a polyisocyanate with a single chiroptical molecular switch covalently linked to the polymer's terminus. (a) Initially, (2′*S*)-(*P*)-**3**-PHIC adopts a *P* helical cholesteric LC phase with a tight pitch. (b) UV irradiation (λ = 365 nm) converts the switchable polymer to (2′*S*)-(*M*)-**3**-PHIC, leading to an elongation of the cholesteric pitch of the LC. (c) Equal amounts of (2′*S*)-(*P*)-**3**-PHIC and (2′*S*)-(*M*)-**3**-PHIC are present in the mixture, resulting in an infinite pitch of the cholesteric LC, which appears as an optically nematic phase. (d) After prolonged UV irradiation, (2′*S*)-(*M*)-**3**-PHIC is present in excess, resulting in the LC matrix returning to cholesteric with inverted helicity (*M*). (e) A PSS is reached, predominantly consisting of (2′*S*)-(*M*)-**3**-PHIC, resulting in an *M* helical cholesteric LC phase with a tight pitch. Irradiation with visible light (λ > 480 nm) leads to a reversal of the process (e → a).

switch cycle as observed before (6.0−3.7 μm). Three subsequent switch cycles, however, did not result in a further decrease in pitch length: similar pitch values, varying between 4.0 and 4.4, were obtained. It is therefore highly unlikely that the observed decrease in pitch length after irradiation is caused by solvent evaporation due to heating of the sample under the irradiation conditions applied, as a gradual further decrease in pitch length over subsequent irradiation cycles would be expected. We propose that the observed tightening of the pitch is actually the result of the photoinduced switching of the polymer's helicity causing an overall improvement in the packing of the polymers in the helical organization of the LC phase. Such an improvement in the packing might well be accompanied by a reduction in the amount of helix reversal points along the polymer chains, leading to the observed tightening of the cholesteric pitch.[51]

In the work described here, we have shown that the preferred helical twist sense of a polyisocyanate can be controlled by a single photochemically bistable chiroptical molecular switch, of which the two thermally stable states are fully addressable with light, which is covalently attached to the polymer's terminus. The hierarchical transmission of chiral information from the molecular level of the chiroptical switch, via the macromolecular level of the helical polymer to the supramolecular level of a cholesteric liquid crystalline phase formed by these helically switchable polymers, allows for the full control of the magnitude and sign of the supramolecular helical pitch of this LC phase using two different wavelengths of light.

(51) This improvement in the packing might also be achieved by applying heating/cooling cycles; in preliminary experiments, however, no significant change in pitch and texture was observed after one heating−cooling cycle (up to 40 °C).

Experimental Section

General Remarks. Chemicals were used as received from Aldrich or Acros; solvents were reagent grade and distilled and dried before use according to standard procedures. Column chromatography was performed on silica gel (Aldrich 60, 230−400 mesh). Uniplate thin-layer chromatography plates were purchased at Analtech (Newark, DE); dimensions, 20 × 20 cm; layer thickness, 2000 μm. ^{1}H and ^{13}C NMR spectra were recorded on a Varian Gemini-200 (50.32 MHz) or on a Varian AMX400 (100.59 MHz) spectrometer in $CDCl_3$. Chemical shifts are denoted in δ-unit (ppm) relative to $CDCl_3$ (^{1}H δ = 7.23, ^{13}C δ = 77). For ^{1}H NMR, the splitting parameters are designated as follows: s (singlet), d (doublet), t (triplet), q (quartet), m (multiplet), and b (broad). For ^{13}C NMR, the carbon atoms are assigned as follows: q (primary carbon), t (secondary carbon), d (tertiary carbon), s (quarternary carbon). MS (EI) and HRMS (EI) spectra were obtained with a JEOL JMS-600 spectrometer. Melting points are taken on a Büchi B-545 melting point apparatus. HPLC analyses were performed on a Shimadzu 10AD-VP system using a Chiralcel AD (Daicel) column. Preparative HPLC was performed on a Gilson HPLC system consisting of a 231XL sample injector, a 306 (10SC) pump, an 811C dynamic mixer, a 805 manometric module, with a 119 UV−vis detector, and a 202 fraction collector, using the Chiralcel AD (Daicel) column. Elution speed was 1 mL/min. UV measurements were performed on a Hewlett-Packard HP 8453 FT spectrophotometer, and CD spectra were recorded on a JASCO J-715 spectropolarimeter using Uvasol-grade solvents (Merck). Irradiation experiments were performed with a Spectroline ENB-280C/FE UV lamp at 365 nm and a 200 W Oriel Xe lamp adapted with a 480 nm cutoff filter. Materials needed for the polymerization: *n*-hexyl isocyanate (Aldrich, 97%) was dried over CaH_2 and vacuum distilled, THF was distilled under N_2 after refluxing with sodium for 5 h. The polymerizations were carried out in a flame-dried Schlenk tube under N_2 atmosphere. GPC measurements were performed on Waters GPC equipment, with THF as solvent and polystyrene as reference, using refractive index and viscosity detection in series and universal calibration via the intrinsic viscosities of the polystyrene reference samples and the polyisocyanates to provide the correct molecular weight distributions.

Preparation and Study of the Liquid Crystalline Phase. The liquid crystalline phase was prepared by dissolving 30 wt % of (2′*S*)-(*P*)-**3**-PHIC in freshly distilled toluene. The liquid crystalline phase was generated between two KBr plates of a liquid IR cell (demountable liquid IR cell as sold by Sigma-Aldrich no. Z112003-1KT). The Teflon spacer placed between the two plates was chosen at a thickness of 200 μm. The liquid crystalline phase images were recorded in transmission using an Olympus BX 60 microscope, equipped with crossed polarizers and a Sony 3CCD DXC 950P digital camera, attached to a personal computer with Matrox Inspector 8.0 imaging software.

7-Bromonaphthalen-2-ol 9. A procedure slightly modified from the one described in ref 31 was followed. To a vigorously stirred mixture of triphenylphosphine (31.5 g, 120 mmol) in MeCN (50 mL), Br_2 (19 g, 6.2 mL, 120 mmol) was added dropwise at 0 °C. The reaction mixture was allowed to reach room temperature, and 2,7-dihydroxynaphthalene **8** (16 g, 100 mmol) was added in one portion. The mixture was heated to 70 °C for 30 min, after which the solvent was removed by rotary evaporation. The flask was equipped with a gas trap, and the black residue was heated to 250 °C for 45 min. After cooling to room temperature, the mixture was dissolved in 200 mL of CH_2Cl_2 and filtered over a plug of silica. The pure product was obtained after column chromatography (SiO_2, pentane/CH_2Cl_2 = 1:1, R_f = 0.22, to pure CH_2Cl_2) as a beige powder (18.6 g, 83.4 mmol, 84%). Mp 127−

129 °C. ^{1}H NMR (400 MHz, $CDCl_3$) δ 5.15 (b, 1H), 7.01 (d, J = 2.6 Hz, 1H), 7.08 (dd, J = 8.8, 2.6 Hz, 1H), 7.37 (dd, J = 8.8, 1.8 Hz, 1H), 7.59 (d, J = 8.4 Hz, 1H), 7.68 (d, J = 8.8 Hz, 1H), 7.79 (d, J = 2.2 Hz, 1H). ^{13}C NMR (100 MHz, $CDCl_3$) δ 108.7 (d), 118.1 (d), 120.8 (s), 127.0 (d), 127.3 (s), 128.3 (d), 129.4 (d), 129.9 (d), 135.7 (s), 154.0 (s). *m*/*z* (EI$^+$, %) = 224, 222 (M$^+$, 100), 115 (38). HRMS (EI$^+$): calcd for $C_{10}H_7{}^{79}BrO$, 221.9680; found, 221.9676. Anal. Calcd for $C_{10}H_7BrO$: C, 53.84; H, 3.16. Found: C, 53.85; H, 3.12.

3-Hydroxy-2-methylpropyl-4-methylbenzenesulfonate 10. To a solution of 2-methyl-1,3-propanediol (9.0 g, 8.9 mL, 0.10 mmol) in $CHCl_3$ (100 mL), pyridine (15.8 g, 16.0 mL, 200 mmol) and *p*-toluenesulfonyl chloride (21 g, 0.11 mol) were added at 0 °C. The stirred solution was allowed to reach room temperature overnight. After addition of water (200 mL), the mixture was extracted with ethyl acetate (3 × 200 mL). The organic extracts were washed with aqueous solutions of HCl (2 M, 100 mL), saturated $NaHCO_3$ (100 mL), and brine, and dried (Na_2SO_4). Evaporation of the solvent yielded a slightly yellow oil. The pure product was obtained after column chromatography (SiO_2, gradient pentane/EtOAc = 2:1, R_f = 0.17, to pure EtOAc), yielding a colorless oil (7.42 g, 31 mmol, 31%). ^{1}H NMR (400 MHz, $CDCl_3$) δ 0.86 (d, J = 7.0 Hz, 3H), 1.95 (m, 1H), 2.39 (s, 3H), 2.68 (b, 1H), 3.43−3.53 (m, 2H), 3.96 (d, J = 5.8 Hz, 2H), 7.30 (d, J = 8.4 Hz, 2H), 7.73 (d, J = 6.6 Hz, 2H). ^{13}C NMR (100 MHz, $CDCl_3$) δ 13.0 (q), 21.5 (q), 35.4 (d), 63.5 (t), 71.9 (t), 127.8 (d), 129.8 (d), 132.7 (s), 144.8 (s). *m*/*z* (CI$^+$, %) = 262 (M + NH_4^+, 100), 108 (2.6).

3-(7-Bromonaphthalen-2-yloxy)-2-methylpropan-1-ol 11. To a stirred solution of **9** (12.7 g, 57.2 mmol) in DMF (500 mL), Cs_2CO_3 (37 g, 114 mmol) and **10** (18 g, 74 mmol) were added, and the mixture was refluxed for 48 h. After cooling to room temperature, the mixture was diluted in ethyl acetate and washed with an aqueous solution of HCl (10%, 3 × 200 mL), saturated $NaHCO_3$ (200 mL), and brine, and dried (Na_2SO_4). After removal of the solvent under reduced pressure, the pure product was obtained after column chromatography (SiO_2, pentane/Et_2O = 2:1, R_f = 0.54) as a white solid (12.4 g, 42 mmol, 74%). Mp 77−79 °C. ^{1}H NMR (400 MHz, $CDCl_3$) δ 1.06 (d, J = 7.0 Hz, 3H), 2.10−2.26 (m, 2H), 3.71 (d, J = 6.9 Hz, 2H), 4.00 (d, J = 6.2 Hz, 2H), 6.99 (d, J = 2.6 Hz, 1H), 7.10 (dd, J = 8.8, 2.6 Hz, 1H), 7.36 (dd, J = 8.4, 1.8 Hz, 1H), 7.57 (d, J = 8.8 Hz, 1H), 7.65 (d, J = 8.8 Hz, 1H), 7.82 (d, J = 2.2 Hz, 1H). ^{13}C NMR (100 MHz, $CDCl_3$) δ 13.6 (q), 35.6 (d), 65.7 (t), 70.8 (t), 105.8 (d), 119.2 (d), 120.5 (s), 126.9 (d), 127.3 (s), 128.6 (d), 129.2 (d), 129.3 (d), 135.7 (s), 157.5 (s). *m*/*z* (EI$^+$, %) = 294, 296 (M$^+$, 30), 222, 224 (100). HRMS (EI$^+$): calcd for $C_{14}H_{15}{}^{79}BrO_2$, 294.0255; found, 294.0243. Anal. Calcd for $C_{14}H_{15}BrO_2$: C, 56.97; H, 5.12. Found: C, 57.15; H, 5.06.

3-(7-Bromonaphthalen-2-yloxy)-2-methylpropanoic Acid 12. To a stirred solution of **11** (8.9 g, 30 mmol) in acetone (250 mL), $KMnO_4$ was added (24 g, 0.15 mol), after which stirring was continued overnight. An aqueous saturated solution of $NaHSO_3$ was added to destroy the excess $KMnO_4$, and the aqueous mixture was acidified by addition of aqueous HCl (10%) and extracted with CH_2Cl_2 (3 × 200 mL). The organic extracts were washed with brine, dried (Na_2SO_4), and the solvent was removed under reduced pressure. The pure product was obtained after column chromatography (SiO_2, EtOAc, R_f = 0.66) as a white solid (5.6 g, 18 mmol, 60%). Mp 156−159 °C. ^{1}H NMR (400 MHz, DMSO-d_6) δ 1.22 (d, J = 7.0 Hz, 3H), 2.90 (m, 1H), 4.12 (dd, J = 9.4, 5.4 Hz, 1H), 4.22 (dd, J = 8.2, 7.0 Hz, 1H), 7.18 (d, J = 9.0 Hz, 1H), 7.36 (s, 1H), 7.45 (d, J = 8.4 Hz, 1H), 7.80 (d, J = 8.8 Hz, 1H), 7.84 (d, J = 9.2 Hz, 1H), 8.07 (s, 1H). ^{13}C NMR (100 MHz, DMSO-d_6) δ 13.8 (q), 38.9 (d), 69.5 (t), 106.2 (d), 119.1 (d), 119.8 (s), 126.5 (d), 127.0 (s), 128.4 (d), 129.4 (d), 129.7 (d), 135.6 (s), 157.1 (s), 175.1 (s). *m*/*z* (EI$^+$, %) = 308, 310 (M$^+$, 48), 222, 224 (100). HRMS (EI$^+$): calcd for $C_{14}H_{13}{}^{79}BrO_3$, 308.0048; found, 308.0063. Anal. Calcd for $C_{14}H_{13}BrO_3$: C, 54.39; H, 4.24. Found: C, 54.40; H, 4.26.

9-Bromo-2-methyl-2,3-dihydro-1*H*-benzo[*f*]chromen-1-one 13. To mechanically stirred polyphosphoric acid (100 mL) at 70 °C, **12** (4.0 g, 13 mmol) was added. The temperature was raised to 110 °C, and the mixture was vigorously stirred for 3 h. After cooling to 70 °C, the reaction mixture was cautiously poured on ice (250 g), and the resulting aqueous solution was stirred at room temperature overnight. The aqueous mixture was extracted with ethyl acetate (4 × 150 mL), the organic extracts were washed with brine and dried (Na_2SO_4), and the solvent was removed under reduced pressure, yielding a brown oil. Further purification could be performed by column chromatography (SiO_2, pentane/EtOAc = 4:1, R_f = 0.8), providing a light-brown solid (2.3 g, 8.0 mmol, 62%). Mp 87−89 °C. ^{1}H NMR (400 MHz, $CDCl_3$) δ 1.21 (d, J = 7.0 Hz, 3H), 2.87 (m, 1H), 4.19 (dd, J = 9.2, 8.8 Hz, 1H), 4.54 (dd, J = 11.3, 5.1 Hz, 1H), 7.01 (d, J = 9.1 Hz, 1H), 7.42 (d, J = 8.4 Hz, 1H), 7.49 (d, J = 8.4 Hz, 1H), 7.75 (d, J = 8.8 Hz, 1H), 9.64 (s, 1H). ^{13}C NMR (50 MHz, $CDCl_3$) δ 11.0 (q), 41.0 (d), 72.0 (t), 110.9 (s), 119.0 (d), 124.5 (s), 127.5 (s), 128.0 (d), 128.1 (d), 129.5 (d), 132.6 (s), 136.7 (d), 163.9 (s), 195.4 (s). *m*/*z* (EI$^+$, %) = 290, 292 (M$^+$, 59), 248, 250 (100). HRMS (EI$^+$): calcd for $C_{14}H_{11}{}^{79}BrO_2$, 289.9942; found, 289.9926. Anal. Calcd for $C_{14}H_{11}BrO_2$: C, 57.76; H, 3.81. Found: C, 57.80; H, 3.77.

Dispiro[9-bromo-2-methyl-2,3-dihydro-1*H*-naphto[2,1-*b*]pyran-1,2′-thiirane-3′,9′′-(9′′*H*)-fluorene] 14. A solution of **13** (500 mg, 1.70 mmol) and P_2S_5 (1.2 g, 5.2 mmol) in benzene (20 mL) was refluxed for 1 h. After cooling to room temperature, the mixture was directly filtered over a plug of silica, eluted with pentane/CH_2Cl_2 = 1:1, to quickly purify the rather unstable thioketone **6**. The first deep-green colored fraction (thioketone **6**) was collected and directly added to a solution of diazofluorenone **7** (660 mg, 3.4 mmol) in toluene (75 mL). The solution was heated at reflux overnight, and after cooling to room temperature, the solvent was removed under reduced pressure. The pure product was obtained after column chromatography (SiO_2, pentane/CH_2Cl_2 = 8:1, R_f = 0.3) as a yellow solid (270 mg, 0.57 mmol, 33%). Mp 177−179 °C. ^{1}H NMR (400 MHz, $CDCl_3$) δ 1.18 (d, J = 6.6 Hz, 3H), 3.13 (m, 1H), 3.61−3.67 (m, 2H), 6.13 (d, J = 7.7 Hz, 1H), 6.54 (t, J = 8.1 Hz, 1H), 6.77 (d, J = 8.8 Hz, 1H), 7.08 (t, J = 8.1 Hz, 1H), 7.32 (t, J = 8.3 Hz, 1H), 7.44 (t, J = 8.2 Hz, 1H), 7.50−7.66 (m, 5H), 7.76 (d, J = 7.3 Hz, 1H), 9.48 (s, 1H). ^{13}C NMR (100 MHz, $CDCl_3$) δ 19.1 (q), 39.6 (d), 53.4 (s), 56.3 (s), 72.4 (t), 116.4 (s), 118.7 (d), 119.4 (d), 120.5 (d), 120.8 (s), 123.5 (d), 124.2 (d), 124.8 (d), 126.0 (d), 126.4 (d), 126.6 (d), 127.6 (d), 127.7 (s), 128.4 (d), 129.5 (d), 130.4 (d), 135.5 (s), 140.0 (s), 141.9 (s), 142.8 (s), 142.9 (s), 155.9 (s). *m*/*z* (EI$^+$, %) = 470, 472 (M$^+$, 45), 438, 440 (100). HRMS (EI$^+$): calcd for $C_{27}H_{19}{}^{79}BrOS$, 470.0340; found, 470.0358.

9-Bromo-1-(9*H*-fluoren-9-ylidene)-2-methyl-2,3-dihydro-1*H*-benzo[*f*]chromene 5. A solution of episulfide **10** (0.30 mg, 0.64 mmol) and triphenylphosphine (0.83 g, 3.2 mmol) in toluene (20 mL) was heated at reflux overnight. After removal of the solvent under reduced pressure the alkene was purified by column chromatography (SiO_2, pentane/CH_2Cl_2 = 8:1, R_f = 0.41), yielding a yellow solid (0.25 g, 0.57 mmol, 89%). Mp 176−177 °C. ^{1}H NMR (400 MHz, $CDCl_3$) δ 1.41 (d, J = 7.0 Hz, 3H), 4.20 (m, 1H), 4.37−4.44 (m, 2H), 6.47 (d, J = 8.1 Hz, 1H), 6.74 (t, J = 7.7 Hz, 1H), 7.12−7.18 (m, 2H), 7.32−7.41 (m, 3H), 7.62 (d, J = 8.8 Hz, 1H), 7.68 (d, J = 7.3 Hz, 1H), 7.76 (d, J = 8.8 Hz, 1H), 7.81 (d, J = 7.0 Hz, 1H), 7.92−7.94 (m, 2H). ^{13}C NMR (100 MHz, $CDCl_3$) δ 15.8 (q), 32.8 (d), 72.5 (t), 113.1 (s), 118.6 (d), 119.1 (d), 120.0 (d), 121.9 (s), 124.5 (d), 125.0 (d), 126.6 (d), 126.8 (d), 126.9 (d), 127.3 (d), 127.4 (d), 127.5 (s), 127.6 (d), 129.8 (d), 131.5 (d), 133.0 (s), 133.1 (s), 136.9 (s), 137.4 (s), 138.3 (s), 139.7 (s), 140.8 (s), 154.2 (s). *m*/*z* (EI$^+$, %) = 438, 440 (M$^+$, 100), 423, 425 (14). HRMS (EI$^+$): calcd for $C_{27}H_{19}{}^{79}BrO$, 438.0619; found, 438.0639. Anal. Calcd for $C_{27}H_{19}BrO$: C, 73.81; H, 4.36. Found: C, 73.55; H, 4.28.

***N*-(1-(9*H*-Fluoren-9-ylidene)-2-methyl-2,3-dihydro-1*H*-benzo[*f*]-chromen-9-yl)benzamide 2.** Following the procedure of Yin and Buchwald,[30] a mixture of **5** (0.14 mg, 0.32 mmol), benzamide (96 mg, 0.80 mmol), 4,5-bis(diphenylphosphino)-9,9-dimethyl-xanthene (45 mg, 77 μmol), $Pd_2(dba)_3$ (24 mg, 26 μmol), and Cs_2CO_3 (209 mg, 0.64 mmol) was stirred in dioxane (2 mL) at 100 °C overnight. After the

mixture was cooled to room temperature, it was diluted in CH_2Cl_2 (20 mL) and filtered over a plug of silica. After removal of all volatiles under reduced pressure, the product was further purified by column chromatography (SiO_2, pentane/EtOAc = 4:1, R_f = 0.5), yielding a yellow solid (150 mg, 0.31 mmol, 98%). Mp 180−182 °C. ^{1}H NMR (400 MHz, $CDCl_3$) δ 1.38 (d, J = 7.3 Hz, 3H), 4.19 (m, 1H), 4.35−4.43 (m, 2H), 6.56 (d, J = 8.1 Hz, 1H), 6.75 (t, J = 8.1 Hz, 1H), 7.06 (d, J = 8.8 Hz, 1H), 7.13 (t, J = 7.5 Hz, 1H), 7.27−7.41 (m, 5H), 7.45 (s, 1H), 7.58−7.64 (m, 4H), 7.73−7.82 (m, 3H), 7.89 (d, J = 8.8 Hz, 1H), 8.20 (d, J = 8.8 Hz, 1H). ^{13}C NMR (100 MHz, $CDCl_3$) δ 15.9 (q), 33.1 (d), 72.3 (t), 113.1 (s), 113.8 (d), 117.3 (d), 118.0 (d), 119.0 (d), 119.9 (d), 124.5 (d), 125.1 (d), 126.4 (s), 126.7 (d), 126.9 (d), 127.1 (2×d), 127.2 (d), 127.3 (d), 128.3 (2×d), 129.5 (d), 131.5 (d), 131.7 (d), 132.3 (s), 132.5 (s), 134.8 (s), 137.6 (s), 137.8 (s), 138.1 (s), 138.4 (s), 139.4 (s), 140.7 (s), 154.1 (s), 165.8 (s). m/z (EI$^+$, %) = 479 (M^+, 100), 374 (10). HRMS (EI$^+$): calcd for $C_{34}H_{25}NO_2$, 479.1885; found, 479.1908. Separation of the enantiomers was achieved by CSP-HPLC (Chiralcel OD, heptane/2-propanol = 95:5, flow rate = 1.0 mL/min, retention times: 35.8 min for (2′*S*)-(*P*)-**2** and 40.6 min for (2′*R*)-(*M*)-**2**.

***N*-(1-(9*H*-Fluoren-9-ylidene)-2-methyl-2,3-dihydro-1*H*-benzo[*f*]-chromen-9-yl)-*N*-acetylbenzamide, (2′*S*)-(*P*)-4.** Sodium bis(trimethylsilyl)amide (50 μL of a 1.0 M solution in THF, 50 μmol) was added to a solution of (2′*S*)-(*P*)-**2** (10 mg, 21 μmol) in THF (4 mL) and stirred at −78 °C. After 5 min acetyl chloride (1.6 μL, 1.7 mg, 22 μmol) was added to the mixture, which was stirred another 5 min and allowed to warm to room temperature. The solution was quenched with a saturated aqueous $NaHCO_3$ solution (50 mL), which was then extracted with ether (3 × 75 mL). The organic phase was washed with brine, dried (Na_2SO_4), and the solvent was removed under reduced pressure. The pure product was obtained after preparative TLC (SiO_2, pentane/EtOAc = 8:1, R_f = 0.25), providing a yellow solid (5.3 mg, 11 μmol, 52%). Mp 193−195 °C. ^{1}H NMR (400 MHz, CD_2Cl_2) δ 1.39 (d, J = 7.0 Hz, 3H), 1.62 (s, 3H), 4.18 (m, 1H), 4.40−4.46 (m, 2H), 6.51 (d, J = 8.8 Hz, 1H), 6.64 (t, J = 7.5 Hz, 1H), 7.09−7.15 (m, 2H), 7.20−7.25 (m, 3H), 7.33−7.41 (m, 5H), 7.63−7.67 (m, 2H), 7.82 (d, J = 6.8 Hz, 1H), 7.85−7.89 (m, 2H), 7.94 (d, J = 7.3 Hz, 1H). ^{13}C NMR (100 MHz, CD_2Cl_2) δ 15.7 (q), 24.6 (q), 33.3 (d), 73.0 (t), 114.4 (s), 119.6 (d), 119.7 (d), 120.3 (d), 124.3 (d), 124.9 (d), 125.1 (d), 125.3 (d), 127.0 (d), 127.4 (d), 127.8 (d), 127.9 (d), 128.5 (2×d), 128.8 (2×d), 129.0 (s), 130.3 (d), 131.9 (d), 132.1 (d), 132.9 (s), 133.1 (s), 135.7 (s), 137.9 (2×s), 138.5 (s), 138.6 (s), 140.2 (s), 140.8 (s), 154.7 (s), 173.0 (s), 173.4 (s). m/z (EI$^+$, %) = 521 (M^+, 100), 416 (15). HRMS (EI$^+$): calcd for $C_{36}H_{27}NO_3$, 521.1991; found, 521.1992.

(2′*S*)-(*P*)-3-PHIC. NaH (1 mg, 50% in oil, 21 μmol) was washed with pentane in a Schlenck tube under N_2, after which (2′*S*)-(*P*)-**2** (9 mg, 19 μmol) dissolved in THF (5 mL) was added. After stirring at room temperature for 10 min, the mixture was cooled to −90 °C, and *n*-hexyl isocyanate (0.56 μL, 0.48 g, 3.8 mmol) was added, upon which the mixture slowly turned more viscous. After 45 min, acetyl chloride (18 μL, 20 mg, 0.25 mmol) and pyridine (20 μL, 20 mg, 0.25 mmol) were added to the mixture, which was then allowed to warm to room temperature. The mixture was then poured in MeOH (100 mL), and the precipitated poly(*n*-hexyl isocyanate) was filtered off, washed three times with MeOH, and dried in vacuo, which yielded a yellow solid (340 mg, 71%). ^{1}H NMR (400 MHz, CD_2Cl_2) δ 0.85 (b, 3H), 1.30 (b, 6H), 1.60 (b, 2H), 3.70 (b, 2H), 6.50−8.00 (low-intensity signals: aromatic protons). ^{13}C NMR (100 MHz, $CDCl_3$) δ 14.0 (q), 22.6 (t), 26.2 (t), 28.4 (t), 31.5 (t), 48.5 (t), 156.8 (s). GPC: M_n = 25 850, M_w = 32 650, D = 1.26.

Acknowledgment. Financial support from The Netherlands Foundation for Scientific Research (NWO-CW) and NanoNed is gratefully acknowledged. We thank Ing. E. J. Vorenkamp for performing the GPC analysis and Dr. M. M. Pollard and T. C. Pijper for helpful discussions.

Supporting Information Available: ^{1}H NMR and APT spectra of all compounds, UV−vis spectra for the photoconversion of (2′*S**)-(*P**)-**2** to (2′*S**)-(*M**)-**2** and vice versa, detailed experimental and crystal data for the X-ray structure determination of (2′*S**)-(*P**)-**2** and (2′*S**)-(*M**)-**2**, crystallographic information files (CIF), Eyring plot of thermal helix inversion of **2**, optical micrographs of the LC film at $PSS_{>480}$ during a series of irradiation cycles. This material is available free of charge via the Internet at http://pubs.acs.org.

JA711283C